Decreasing measles burden by optimizing campaign timing

Niket Thakkar[a,1], **Syed Saqlain Ahmad Gilani**[b], **Quamrul Hasan**[c], **and Kevin McCarthy**[a]

[a]Institute for Disease Modeling, Bellevue, USA 98005; [b]Ministry of National Health Services, Regulations, and Coordination, Islamabad, Pakistan; [c]World Health Organization Country Office, Islamabad, Pakistan

This manuscript was compiled on October 25, 2018

Measles remains a major contributor to preventable child mortality, and bridging gaps in measles immunity is a fundamental challenge to global health. In high-burden settings, mass vaccination campaigns are conducted to increase access to vaccine and address this issue. Ensuring that campaigns are optimally effective is a crucial step towards measles eradication; however, the relationship between campaign impact and disease dynamics is poorly understood. Here, we study measles in Pakistan, and we demonstrate that campaign timing can be tuned to optimally interact with local transmission seasonality and recent incidence history. We develop a mechanistic modeling approach to optimize timing in general high-burden settings, and we find that in Pakistan, hundreds of thousands of infections can be averted with no change in campaign cost.

measles eradication | time series | mathematical model | vaccine

Measles is a significant source of global disease burden and child mortality, estimated to have caused 7 million infections and 90 thousand deaths in 2016 (1). Although an effective, safe, and cost-efficient measles vaccine has existed since the 1960's, vaccination in high-burden settings remains a challenge due largely to poor health care infrastructure and access (1–3). As a result, measles vaccine dissemination is a pressing global health and social justice issue.

While routine immunization (RI) at 9 and 15 months of age is the World Health Organization (WHO) recommended vaccination method (2), high-burden settings rely heavily on mass vaccination campaigns, termed supplemental immunization activities (SIAs), to provide measles vaccine more broadly (3). In these campaigns, health-workers advertise and run fixed-post vaccination sites to target all children in a specified age-range with the aim to vaccinate susceptible children missed by RI (3). SIAs are logistically complicated and implementing them successfully requires a combination of operational excellence, planning, and knowledge of region-specific needs. While understanding and optimizing SIA implementation is therefor a difficult general problem, it is a critical contributor to measles burden control and an important step towards global measles eradication.

In this report we analyze measles in Pakistan, a high-burden setting (4), and show that SIA impact is strongly dependent on timing. We present a general time-series susceptible-infected-recovered (TSIR) model (5) which explicitly accounts for SIAs in the process of inferring underlying susceptible population, transmission seasonality, and future infections. Fitting this model to lab-confirmed measles cases from 2012-2017, we show that Pakistan has significant annual measles transmission seasonality with a high season beginning in October and continuing through the following April. This seasonality has implications for SIA timing, and using the model to extrapolate from 2018-2021, we show that an SIA conducted in November prevents on average $\sim 400,000$ more infections than an equivalent campaign run in January. Finally, by extending the model to province-level, we show that optimal SIA timing is spatially heterogeneous, and we discuss implications of this result for future SIA planning in Pakistan and elsewhere.

Measles transmission seasonality in Pakistan. Measles is a highly virulent disease, and lab-confirmed measles cases in Pakistan have more than doubled from 2016 to 2017 (4). Pakistan's most recent Demographic and Health Survey (DHS, 2012-13) estimates measles vaccination coverage in 1 to 2 year-olds at 61.4% nation-wide, with significant sub-national heterogeneity (26.4% to 85.2%) (6). Given this relatively low RI coverage, informed and effective SIAs are needed to slow and potentially interrupt measles transmission.

Mechanistic modeling allows us to understand measles seasonality while estimating underlying susceptible populations and forecasting policy outcomes. TSIR models of measles are well-studied (7–10) and have been used to understand measles transmission in a variety of settings (11, 12). While modern TSIR methods typically use Markov-Chain Monte Carlo (13) or related algorithms (14, 15) to calibrate to incidence data, we forgo this complexity and instead extend the more robust linear-regression approach (5) to the high-burden context by incorporating past interventions.

Considering time in semi-monthly increments corresponding to a measles infection's typical duration (1, 16), we model S_t, the susceptible population at time t, and I_t, the correspond-

Significance Statement

Measles vaccine is a highly effective health-care intervention, but getting vaccine to those in need remains a major problem. Complicating the issue, high-burden countries typically have low-quality infrastructure, severely limiting the number of infections detected and therefore limiting our understanding of local epidemiology. Here we show that statistical disease models can be fit to sparse case data from Pakistan using a robust linear regression approach. This method yields estimates of the effects of past interventions, the seasonal likelihood of measles transmission, and the magnitude of future outbreaks under different intervention policies. We use these models to understand in general when and where vaccine should be distributed to prevent as many measles cases as possible.

N.T. developed the modeling approach, analyzed the results, and wrote the manuscript. S.G. and Q.H. formulated the research project and were responsible for data collection. K.M. supervised the research and assisted model development. Both Q.H. and K.M. edited the manuscript.

The authors declare no competing interests.

[1]To whom correspondence should be addressed. E-mail: nthakkar@idmod.org

ing infection prevalence at time t, as a discrete, stochastic dynamical system,

$$S_t = (1 - \mu_{t-1})(B_t + S_{t-1} - I_t) \quad [1]$$

$$I_t = \beta_t I_{t-1}^{\alpha} S_{t-1} \varepsilon_t \quad [2]$$

$$C_t \sim \text{Binom}\{I_t, p\}. \quad [3]$$

Here, B_t is an assumed known estimate of births missed by RI at time t, μ_t is the fraction of susceptible population reached by any SIA at time t, α models inhomogeneous population mixing (5), and β_t is the average number of infectious contacts per person at time t which we assume has an annual periodicity. Transmission uncertainty is accounted for by ε_t, a zero-mean, log-normal random process, and lab-confirmed cases, C_t, are assumed to be drawn from a binomial distribution where p is the lab-reporting-rate, an unknown probability for cases to be selected for lab study. In Eq. 1 children missed by RI, B_t, contribute to S_t while infections and SIAs serve to decrease S_t. Simultaneously, Eq. 2 models new infections occurring at rate β_t as infectious and susceptible populations interact.

Since measles SIAs happen relatively infrequently, Pakistan's campaign history can be used to reduce μ_t to the estimation of a single parameter. Sub-national vaccination campaigns have been conducted 6 times in Pakistan since 2012 with wide variation in target population (17). Here we assume that non-zero $\mu_t = P_t \mu$ where P_t is the known target population fraction and μ is an unknown SIA efficacy parameter common to all campaigns from 2012-2017.

Given the observed C_t series and corresponding B_t (via RI coverage estimates (6) and birth-rate estimates (18–20), see Methods), the model can be fit to data in a two-step linear regression process described in the Methods and Supplementary Section 2. Model calibration yields estimates of α, μ, p, and β_t with uncertainty due both to under-reporting and transmission stochasticity.

Fitting the model to national-level reports yields $p = 0.23 \pm 0.04\%$, indicating, in qualitative agreement with similar estimates from high-burden settings (21), that a single lab-confirmed case corresponds on average to ~ 400 infections in the population. Simultaneously, we find $\alpha = 0.93 \pm 0.03$, indicating that inhomogeneous population mixing is a small but statistically significant effect. Past SIA efficacy μ is estimated to be 40% which shows that campaign efforts have had a significant effect on measles susceptibility in Pakistan.

In Fig. 1, national-level reports from 2012-2017 are aggregated by month (gray bars) showing that the majority of measles cases occur in the first half of the year. The inferred β_t consistent with this case distribution is averaged by month and overlaid in red (standard deviation cloud), showing that low transmission occurs between May and October (blue), Pakistan's hot, summer rainy season. This correlation between measles transmission and rainfall or temperature agrees with findings from research in other settings (11, 22) and suggests that transmission fluctuates due to seasonal population migration and related annual variation in contact-rates (23).

Interestingly, the increase in transmission precedes the rise in cases by 2 to 3 months. This phase difference is in quantitative agreement with seasonality studies of measles in the pre-elimination U.S. (24), suggesting that although a measles infection's duration is only 2 to 3 weeks, high transmission is required for considerable time before enough infections have occurred to spark an outbreak. Operationally speaking, this

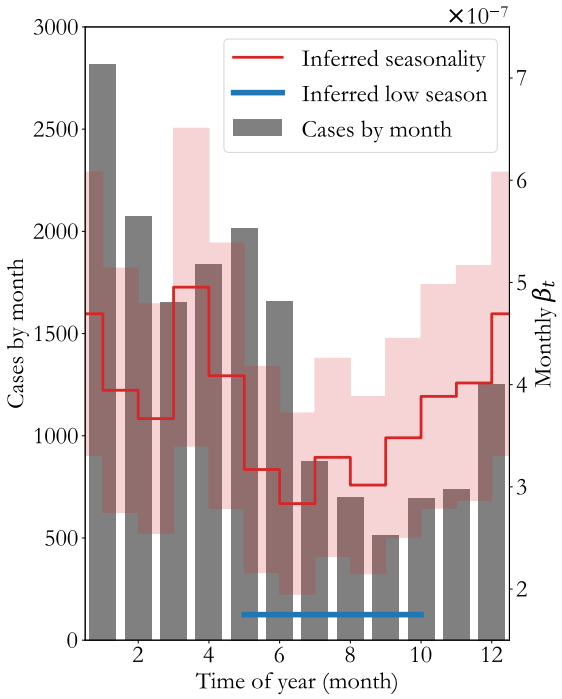

Fig. 1. Measles transmission seasonality in Pakistan. Lab confirmed cases from 2012-17 aggregated by month are plotted as gray bars. The corresponding inferred force of infection (red trace, standard deviation cloud) shows that transmission varies by as much as 50% throughout the year, with a low season (blue line) from May through September, Pakistan's summer rainy season.

is a valuable insight since lows in the aggregated case-count alone might incorrectly suggest that Pakistan's low measles transmission season ranges from July to November.

Model seasonality and corresponding extrapolation ability are tested against lab-reporting-rate scaled cases (black dots) in Fig. 2. In red, predicted I_t given C_{t-1} shows that the model is capable of reliable semi-monthly prediction with relatively low uncertainty (red cloud, 95% CI). A more substantial test of the model is shown in black, where I_t is predicted for a full 6 years starting with C_0 in January 2012. This long-term model prediction has larger uncertainty (grey cloud, 95% CI) as expected and captures the major outbreaks in 2013, 2016, and 2017, demonstrating that the inferred seasonality is consistent with the observed dynamics. The corresponding inferred S_t is plotted in blue showing stark decreases in susceptible population following SIAs (gray dashed lines) with heterogeneity between SIAs due largely to differences in target population.

Optimal SIA timing. An effective vaccination campaign immunizes susceptible individuals in order to stifle measles transmission before it occurs. SIAs accomplish this in the model by both decreasing S_t in Eq. 1 and the resulting I_t in Eq. 2. Intuitively, based on the seasonality of Fig. 1, we expect that SIAs in Pakistan will have greatest impact in October or November since susceptible population built-up over the summer low-season can be immunized before high transmission begins. Using the model, we demonstrate that this intuition is qualitatively correct, but a given population's recent measles history also effects optimal SIA timing.

Hypothetical SIA policies can be quantitatively compared

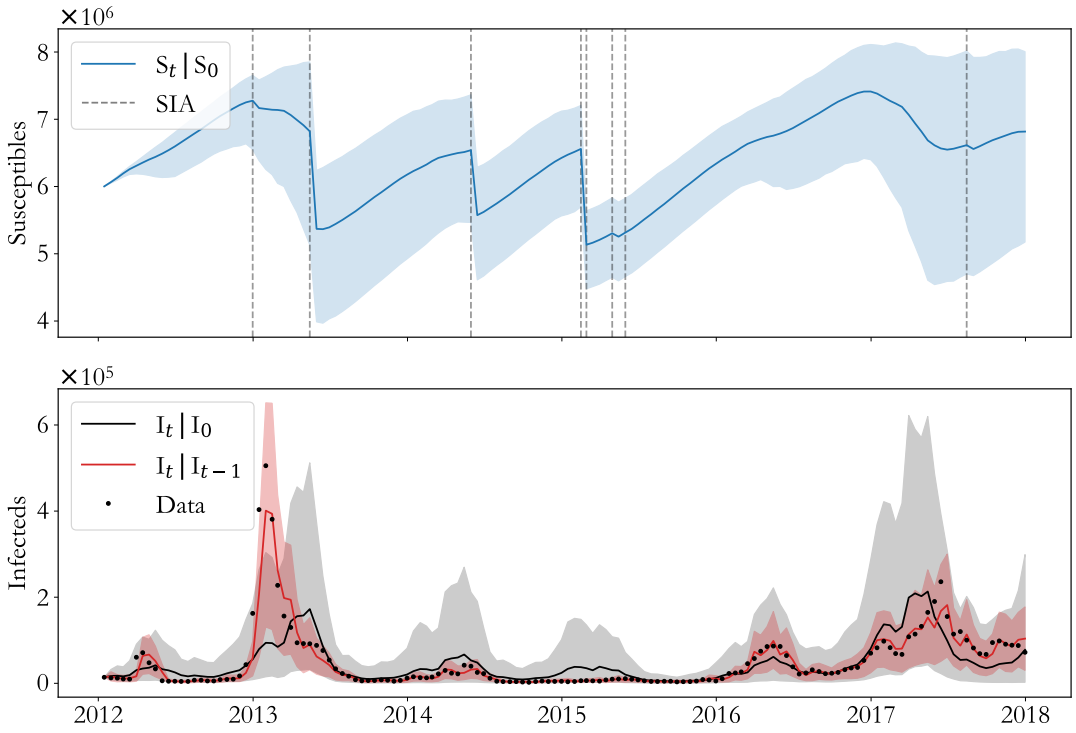

Fig. 2. Testing model performance. In the lower panel, semi-monthly (red) and 6-year (black) model extrapolations are compared to lab-reporting-rate scaled cases demonstrating that the model predicts outbreak timing and magnitude. In the upper panel, the underlying susceptible population (blue) corresponding to the long-term projection highlights the potentially strong effect of SIAs (gray dashed lines). For all traces, shaded regions indicate 95% confidence intervals (CIs).

by calculating projected infections. Here, we focus on SIAs run in 2018 over the course of a full month with half the population targeted in each semi-monthly model period, and we compute the sample distribution of total infections from 10000 model runs starting with the data at the end of 2017 and forecasting for 3 years. The 2018-2021 forecasting period was selected since, in practice, multiple SIAs will be run in > 3 year periods, and we are interested in comparing effects of single SIAs for simplicity. All hypothetical campaigns have efficacy equal to the inferred 2012-2017 efficacy, $\mu = 40\%$, in order to isolate the effects of SIA timing.

Expected infections under hypothetical 2018 SIA policies are plotted in black in Fig. 3(a). As anticipated based on the seasonality, a November SIA has greatest impact, with ~ 440000 less infections on average than an otherwise equivalent campaign run in January. Moreover, if the extra 10 months to prepare leads to increases in SIA efficacy, we find that November rapidly becomes even more strongly favored (Supplementary Fig. 6). Throughout the low transmission season (shaded blue region), campaigns become more-and-more effective. This is as we would expect since susceptible population build-up results in a wider-reaching campaign with greater herd-immunity effects.

As a direct consequence of this however, delays past November rapidly incur large costs since the 2018-2019 high transmission season depletes the susceptible population and mitigates the effect of an SIA. This is demonstrated in Fig. 3(a) by extending the analysis to equivalent campaigns in 2019. Expected infections under these policies are plotted in red, and we find that a campaign delayed from November 2018 to May 2019 results in over 600000 more measles infections on average over the 2018-2021 period.

Fig. 3(b) plots extrapolated model traces for SIAs before (in April, blue) and after (in November, green) the 2018 low-transmission season for more detailed comparison. While the April SIA mitigates infections in 2018, this comes at the expense of a large outbreak in 2020. On the other hand, the November SIA decreases the severity of the predicted 2020 outbreak at the expense of infections in 2018. This trade-off indicates that transmission seasonality's contribution to the optimal SIA timing acts in concert with the expected severity of upcoming outbreaks, an expectation which depends directly on measles' recent history in a population. For Pakistan as a whole, 2017 was a relatively severe measles year, indicating that natural infection has decreased the susceptible population. Consistent with this intuition, model extrapolation predicts that 2020's outbreak will be larger on average than 2018's, and the November SIA is preferable as a result.

The interplay between seasonality and recent history is highlighted if we apply the model to Pakistan's provinces individually. To do this, the model is fit to province-level data assuming the national-level transmission seasonality of Fig. 1 with a contact-rate scaled by the fraction of Pakistan's population within the province. The assumption that measles transmission behaves qualitatively similarly across the country is necessary since individual provinces report too few lab-confirmed cases to reliably infer province-level transmission parameters. Province-level models are tested by the methods of Fig 2 in Supplementary Section 4. They show comparable predictive performance to the national-level model indicating

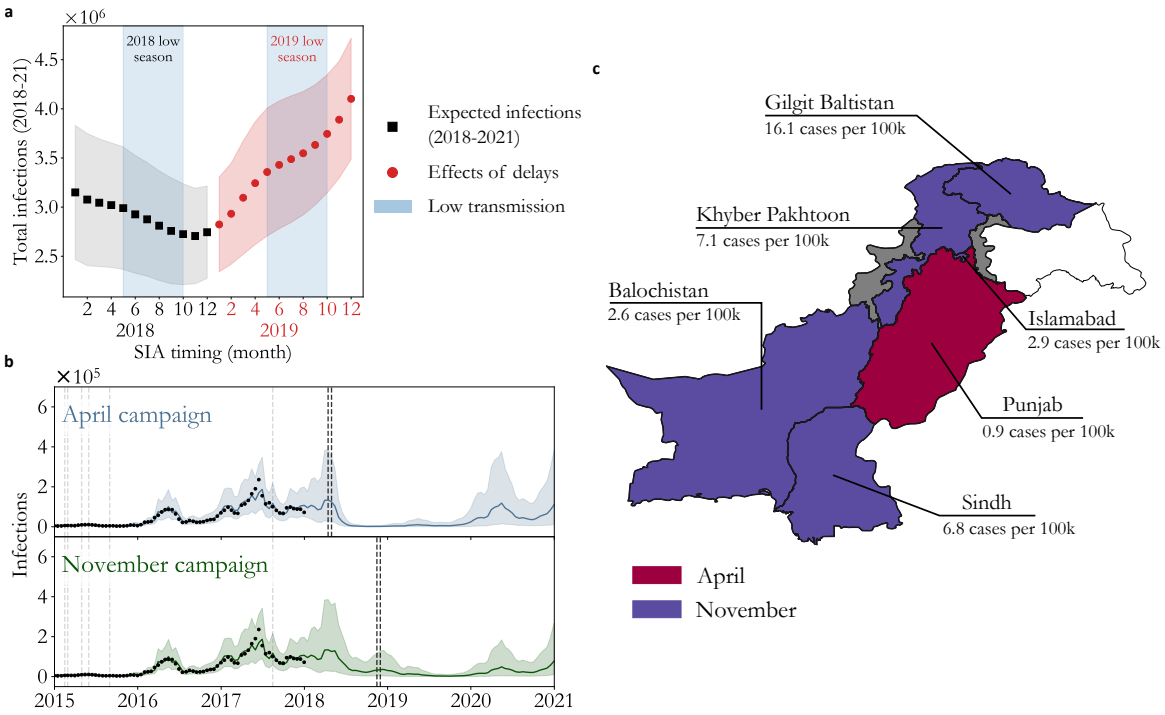

Fig. 3. Optimizing SIA timing in Pakistan. (a) Comparing total expected infections in 2018-2021 (black, standard error shading) under different SIA policies shows that November minimizes measles burden by taking advantage of susceptible build-up over the low transmission season (blue region). As a result however, delays into the 2018-19 high transmission season (red, standard error shading) are costly. (b) Model projections for pre- (April) and post-low-transmission season (November) SIAs (black dashed lines) demonstrate the trade-off between 2018 and 2020 outbreak control. As a result, 2017 measles burden also plays a significant role in timing optimization. (c) Extending the model to province-level allows us to compare April and November SIA timing sub-nationally. Preference for April is mapped in red while preference for November is mapped in purple; grey provinces (FATA and Azad Kashmir, representing less than 5% of Pakistan's total population (20)) are inaccessible to health workers while white areas indicate disputed territory. Heterogeneity in the 2017 lab-confirmed measles cases per 100k (indicated) is reflected in the timing optimization.

that the seasonality assumptions are valid.

Sub-nationally, Pakistan's recent measles history has significant heterogeneity. For example, in Pakistan's two most populated provinces, Punjab and Sindh, lab-confirmed measles cases per 100000 in 2017 were at 0.9 and 6.8 respectively. While this is due in part to RI coverage differences between Punjab and Sindh (6), this also indicates that 2017 was an outbreak year in Sindh but not Punjab. This heterogeneity is mirrored in province-level optimal SIA timing: Comparing April and November SIAs where data is available, we see in Fig. 3(c) that in provinces with high 2017 case counts the November campaign is more effective (purple) while in Punjab the April SIA performs better (red). Thus, in-line with intuition from the national level, optimizing SIA timing requires a balance between contributions due to seasonality and incidence history. The modeling approach presented here offers a robust means to solve this optimization problem in high-burden contexts.

Discussion

Measles vaccination campaign optimization is a complex general problem. Here, we have studied data from Pakistan to demonstrate that SIA timing is a critical factor, and that two SIAs with equivalent efficacy and cost may have significantly different impact solely as a result of their start date. With that in mind, transmission-seasonality and recent measles burden, the drivers of optimal campaign timing, should be considered alongside operational constraints in future SIA planning.

From a methodological perspective, the TSIR model used in this work is a robust tool for evaluating competing SIA polices. While disease models with mass vaccination have been studied in the past (25–27), generalization of a least-squares-based model calibration method (5) to the high-burden context offers a simple, data-driven SIA optimization approach. Model extensions such as age-structure (28), sub-national spatial correlation (10), and disease importation (7) are active areas of research. These studies, in conjunction with the method presented here, may contribute to other aspects of SIA optimization, an important problem for measles eradication with widespread global health implications.

Methods

Pakistani demographic and surveillance data. Population estimates for 2010 and 2015 and live-birth estimates for 2010, 2012, 2015, and 2020 were obtained from WorldPop (18–20). These were aggregated to district level and linearly interpolated over time. Rates for the first dose of measles vaccine were estimated using the 2012-13 DHS (6) and treated as constant over the 2012-2017 model period.

Lab-confirmed and rejected cases were obtained from Pakistan's WHO affiliated lab. The rejected cases and corresponding self-reported dose histories were used to estimate rates of second dose measles vaccine coverage in all provinces. Combining these estimates of demographic quantities gives

$$B_t = \tilde{B}_t \left[1 - 0.9V_{1,t}(1 - V_{2,t}) - 0.99V_{1,t}V_{2,t}\right],$$

where $V_{1,t}$ and $V_{2,t}$ are first and second dose measles vaccine coverage over time, and $\tilde{B}_t$ is the estimated live-births. The

above model assumes the first vaccine dose has a 90% seroconversion rate and the second dose has a 99% seroconversion rate (16). For more details, see Supplementary Section 1.

Fitting and testing the model. Model fitting to an observed C_t series proceeds in two steps accounting for uncertainty due to under-reporting and transmission individually. In the first step, Eq. 1 is used to construct a weighted least squares regression of B_t against C_t which yields, for a given μ_t, estimates of p and the relative fluctuations in the susceptible population. Further assuming that susceptible fluctuations are small and $\beta_t = \beta_{t\mathrm{mod}24}$, i.e. that seasonality varies only within a year, Eq. 2 defines a generalized linear auto-regression of I_t. Solving this regression problem yields estimates of β_t and the remaining parameters including the variance due to transmission uncertainty.

As mentioned in the main text, we assume $\mu_t = \mu P_t$ where P_t is a known measure of target SIA population (29) and μ is an efficacy parameter common to all SIAs from 2012-2017. Since regression approach above can be carried out given a hypothetical μ, we take an approach similar to the profile likelihood optimization used by others (14, 15). In other words, a range of μ are tested by repeated model fitting and subsequent goodness-of-fit optimization. For mathematical details of the full model calibration procedure and related sensitivity testing see Supplemental Section 2.

Acknowledgements. The authors would like to thank the Pakistan's Expanded Program on Immunization for providing the lab reported data, Kurt Frey for useful conversations and significant help with compiling Pakistan's past SIA calendar, Hil Lyons for assistance with computing birth rates from the DHS, and Caitlin Cornell for useful edits to the manuscript.

1. (2018). World Health Organization, "Measles Fact Sheet", (http://www.who.int/mediacentre/factsheets/fs286/en/).
2. (2017). World Health Organization, "Summary of the WHO position on measles vaccine", (http://www.who.int/immunization/policy/position_papers/measles/en/).
3. (2016). World Health Organization. "Planning and implementing high-quality supplementary immunization activities for injectable vaccines", (http://www.who.int/immunization/diseases/measles/en/).
4. (2017). World Health Organization, "Measles cumulative report for 2017", (http://www.emro.who.int/vpi/publications/measles-monthly-bulletin.html).
5. Finkenstädt BF, Grenfell BT (2000) Time series modelling of childhood diseases: a dynamical systems approach. *Journal of the Royal Statistical Society: Series C (Applied Statistics)* 49(2):187–205.
6. (2013). National Institute of Population Studies - NIPS/Pakistan and ICF International, "Pakistan Demographic and Health Survey 2012-13".
7. Grenfell B, Bjørnstad O, Kappey J (2001) Travelling waves and spatial hierarchies in measles epidemics. *Nature* 414(6865):716.
8. Bjørnstad ON, Finkenstädt BF, Grenfell BT (2002) Dynamics of measles epidemics: estimating scaling of transmission rates using a time series sir model. *Ecological Monographs* 72(2):169–184.
9. Grenfell BT, Bjørnstad ON, Finkenstädt BF (2002) Dynamics of measles epidemics: scaling noise, determinism, and predictability with the TSIR model. *Ecological Monographs* 72(2):185–202.
10. Xia Y, Bjørnstad ON, Grenfell BT (2004) Measles metapopulation dynamics: a gravity model for epidemiological coupling and dynamics. *The American Naturalist* 164(2):267–281.
11. Ferrari MJ, et al. (2008) The dynamics of measles in sub-Saharan Africa. *Nature* 451(7179):679.
12. Dalziel BD, et al. (2016) Persistent chaos of measles epidemics in the prevaccination United States caused by a small change in seasonal transmission patterns. *PLoS computational biology* 12(2):e1004655.
13. Morton A, Finkenstädt BF (2005) Discrete time modelling of disease incidence time series by using Markov chain Monte Carlo methods. *Journal of the Royal Statistical Society: Series C (Applied Statistics)* 54(3):575–594.
14. Ramsay JO, Hooker G, Campbell D, Cao J (2007) Parameter estimation for differential equations: a generalized smoothing approach. *Journal of the Royal Statistical Society: Series B (Statistical Methodology)* 69(5):741–796.
15. Ionides EL, Nguyen D, Atchadé Y, Stoev S, King AA (2015) Inference for dynamic and latent variable models via iterated, perturbed Bayes maps. *Proceedings of the National Academy of Sciences* 112(3):719–724.
16. Plotkin S, Orenstein W, Offit P, Edwards KM (2017) *Plotkin's Vaccines.* (Elsevier), 7 edition.
17. (2018). World Health Organization, "Summary of Measles-Rubella Supplementary Immunization Activites, 2000-2018", (http://www.who.int/immunization/monitoring_surveillance/data/en/).
18. Tatem AJ (2017) Worldpop, open data for spatial demography. *Scientific data* 4:170004–170004.
19. Tatem AJ, et al. (2014) Mapping for maternal and newborn health: the distributions of women of childbearing age, pregnancies and births. *International journal of health geographics* 13(1):2.
20. Gaughan AE, Stevens FR, Linard C, Jia P, Tatem AJ (2013) High resolution population distribution maps for Southeast Asia in 2010 and 2015. *PloS one* 8(2):e55882.
21. Simons E, et al. (2012) Assessment of the 2010 global measles mortality reduction goal: results from a model of surveillance data. *The Lancet* 379(9832):2173–2178.
22. Altizer S, et al. (2006) Seasonality and the dynamics of infectious diseases. *Ecology letters* 9(4):467–484.
23. Bharti N, et al. (2011) Explaining seasonal fluctuations of measles in Niger using nighttime lights imagery. *Science* 334(6061):1424–1427.
24. Yorke JA, Nathanson N, Pianigiani G, Martin J (1979) Seasonality and the requirements for perpetuation and eradication of viruses in populations. *American Journal of Epidemiology* 109(2):103–123.
25. d'Onofrio A (2002) Pulse vaccination strategy in the SIR epidemic model: global asymptotic stable eradication in presence of vaccine failures. *Mathematical and Computer Modeling* 36(4-5):473–489.
26. Gao S, Chen L, Nieto JJ, Torres A (2006) Analysis of a delayed epidemic model with pulse vaccination and saturation incidence. *Vaccine* 24(35-36):6037–6045.
27. Briat C, Verriest EI (2009) A new delay-SIR model for pulse vaccination. *Biomedical signal processing and control* 4(4):272–277.
28. Kuniya T (2011) Global stability analysis with a discretization approach for an age-structured multigroup SIR epidemic model. *Nonlinear Analysis: Real World Applications* 12(5):2640–2655.
29. (2017). World Health Organization. "Summary of measles-rubella supplementary immunization activities", (http://www.who.int/immunization/monitoring_surveillance/data/en/).